Modulation of the immunogenicity of a Rift Valley fever virus DNA vaccine by ELR nanocarriers

Juan Gonzalez-Valdivieso[1], Belén Borrego[2], Alessandra Girotti[1], Sandra Moreno[2], Alejandro Brun[2], Jesus F. Bermejo-Martin[3,4] and F. Javier Arias[1*].

[1] BIOFORGE (Group for Advanced Materials and Nanobiotechnology), CIBER-BBN, University of Valladolid, Paseo de Belén 19, 47011, Valladolid, Spain.

[2] Instituto Nacional de Investigación y Tecnología Agraria y Alimentaria (INIA), Centro de Investigación en Sanidad Animal (CISA), Valdeolmos, 28130 Madrid, Spain.

[3] Laboratory of Biomedical Research in Sepsis (BioSepsis), Hospital Universitario Río Hortega, Calle Dulzaina, 2, 47012 Valladolid, Spain

[4] Institute for Biomedical Research of Salamanca (IBSAL), Paseo de San Vicente, 58-182, 37007 Salamanca, Spain

[*]Corresponding author: arias@bioforge.uva.es

Abstract

This work analyzes the immunogenicity of six genetically engineered constructs based on Elastin-Like Recombinamers (ELRs) fused to the Gn glycoprotein from Rift Valley fever virus (RVFV). Upon transfection, all constructs showed no effect on cell viability. While fusion constructs including ELR blocks containing hydrophobic amino acids (alanine or isoleucine) did not increase the expression of viral Gn in eukaryotic cells, glutamic acid- or valine-rich fusion proteins showed enhanced expression levels

compared to the constructs encoding the viral antigen alone. However, *in vivo* DNA plasmid immunization assays determined that the more hydrophobic constructs reduced viremia levels after RVFV challenge to a higher extent that glutamic or valine-rich encoding plasmids and were better inducers of cellular immunity as judged by *in vitro* re-stimulation experiments. Although the Gn-ELR fusion constructs did not surpass the protective efficacy of a plasmid vaccine expressing non-fused Gn, our results warrant further experiments directed to take advantage of the immunomodulatory potential of ELR biomaterials for improving vaccines against infectious diseases.

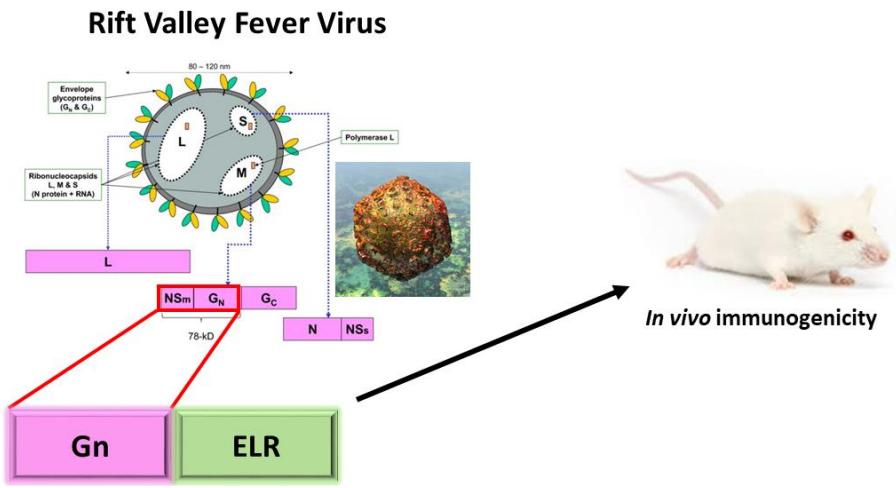

Keywords: Rift Valley fever virus, DNA vaccines, Elastin-Like Recombinamers (ELRs), Vaccine technologies, *In vivo* immunogenicity.

1. Introduction

Novel biomaterials have emerged as a useful tool for multiple biomedical applications [1]. Among the most promising biomaterials we find Elastin-like polypeptides (ELPs), polymers formed by short pentapeptide VPGXG repeats found in natural elastin sequence where X can be any amino acid except proline [2]. A new term, elastin like

recombinamers (ELRs), has been designed to refer to ELPs biosynthesized by using genetic engineering techniques [3-4]. ELRs-based biomaterials are becoming increasingly important in different fields of biomedicine, as regenerative medicine or drug and gene delivery [5-7]. Recombinant DNA technology allows us to produce ELRs with absolute control over the sequence, and the capability of including different functionalities and bioactive sequences [8]. ELRs, due to their biological origin and properties, possess characteristic features that make them an interesting alternative for biomedical applications, such as biocompatibility, biodegradability and environmentally responsive behavior [9]. Garcia-Arevalo *et al*. developed ELR-based nanovaccines in order to present antigenic peptides from *M. tuberculosis* and achieve long half-life of the presented antigen in circulation. *In vivo* immune-challenge experiments demonstrated the induction of a biphasic response consisting on the early secretion of chemotactic cytokines, then followed by the induction of a Th-2 immune response [10].

One of the main disadvantages of therapeutic proteins resides in their short circulating half-lives, which means that frequent administration or high concentration to achieve effective levels are needed [11]. However, ELRs have been described as promising pharmacokinetic enhancers in order to prolonged half-life and stability of peptides as these new biomaterials are able to improve the pharmacokinetic profile and biodistribution of a peptide compared to the free molecule, resulting therefore in specific delivery of the therapeutic agent [1-2].

DNA vaccination is based on plasmids encoding genes of relevant vaccine antigens under control of eukaryotic promoter sequences, such as the human cytomegalovirus immediate-early promoter (hCMV) [12]. Thus, the foreign antigen is produced by the host cells, therefore mimicking the replication of live pathogens and stimulating both

humoral and cellular immune responses [13,14]. Furthermore, the structure and post translational modifications of the antigen are maintained. Moreover, the genetic engineering techniques allow us to develop a wide library of antigens when designing vaccine combinations in order to modulate or improve the immune response induced in the host animal [15]. This approach has been used for the development of therapeutic treatments for cancer, auto-immune diseases and allergies, as well as for vaccines against emerging infectious diseases caused by bacteria or viruses [16-17].

An important target for which DNA vaccines have shown promise is Rift Valley fever virus (RVFV). RVFV is a negative strand RNA virus that belongs to the genus *Phlebovirus* (family *Phenuiviridae*, order *Bunyavirales*) and causes an important disease in wild and domesticated ruminants, resulting in high rates of morbidity, mortality and abortion, and is often transmitted to humans [18-19]. This virus is transmitted by bite of many different mosquito species, as well as by direct contact with body fluids from viremic animals and inhalation of aerosols [20]. The disease caused by this pathogen, Rift Valley fever (RVF), is endemic in sub-Saharan Africa, Egypt and Saudi Arabia. In the sub-equatorial Africa outbreaks are cyclic and are linked to heavy rainfalls that allow the establishment of mosquito breeding areas [21]. More recently, the disease has occurred in different places, such as Egypt, the Arabian Peninsula, Madagascar, Indian Ocean islands and Mayotte, which confirms that this disease has a wide potential to spread all over the world. In addition, the risk of virus introduction to disease-free areas such as Europe or America could be increased by phenomena associated with climate change as well as the rise in international trade of animals [22]. These facts and the wide host range of the virus and high vector competence of numerous mosquito species could

facilitate the outbreaks of the disease with unpredictable consequences for public and animal health [23-24].

The virus is composed by a tripartite genome, which comprises large (L), medium (M) and small (S) segments [25]. First, the L segment encodes a RNA-dependent RNA polymerase (RdRp) whose role involves transcription and replication of the viral genome. The M segment encodes two structural glycoproteins (Gn and Gc) as well as the accessory proteins: a 13–14 kDa anti-apoptotic protein (NSm) and a 78 kDa protein [26]. Both Gn and Gc glycoproteins are responsible of host cell receptor binding and fusion, hence constituting the major structural antigens and main targets for neutralizing antibodies. Finally, the S segment encodes two different genes: the viral nucleoprotein N, which is associated with the viral RNA to form the nucleocapsid, and the non-structural protein NSs, which is associated with virulence [27].

Vaccination is the only effective strategy for the control and prevention of this disease [28-29]. Unfortunately, currently available vaccines are based on attenuated or inactivated virus that retain important disadvantages, such as low immunogenicity and adverse side effects resulting in teratogenicity and abortions, that preclude their use in non-endemic countries [30]. For this reason, developing new generation RVF vaccines based on recombinant proteins, Virus-Like Particles (VLPs), recombinant viral vectors or DNA-based vaccines has been the subject of intense research activities in recent years aimed to achieve safer vaccines capable of inducing a rapid and long-lasting immune response with potential use for both human and veterinary purposes.

The RVFV glycoprotein Gn carries determinants for both neutralizing antibody induction and cell-mediated immune responses [21, 31-32] so it is often the antigen of choice in different vaccine formulations including subunit or DNA vaccines [33-34]. In this work, we have developed DNA plasmids encoding several RVFV-Gn-ELR fusion constructs in order to test their production, immunogenicity and vaccine potential against RVFV challenge in an *in vivo* mouse model.

2. Material and methods

2.1 Chemical Reagents and Cell Lines

Primers for mutagenesis and DNA sequencing were acquired from Metabion. Genes for ELR sequences were available from BIOFORGE group library. QuickChange Site-Directed Mutagenesis Kit was purchased form Stratagene. *Pfu* Turbo DNA Polymerase was supplied by Agilent. Simply Safe nucleic acid stain was acquired from Eurx. Endo Free Plasmid Maxi Kit was supplied by Qiagen. Turbofect Transfection Reagent was purchased from Fermentas. 293T human embryonic kidney cells (CRL-3216), BHK-21 (C-13) hamster kidney fibroblasts (CCL-10) and African green monkey kidney cells (Vero cells, CCL-81) were supplied by American Type Culture Collection (ATCC). S.O.C. Medium, XL-1 Blue competent cells, 1 Kb Plus DNA Ladder, Lipofectamine LTX Plus Reagent, Dulbecco's Modified Eagle's Medium (DMEM), Eagle's Minimum Essential Medium (EMEM), Fetal Bovine Serum (FBS), penicillin-streptomycin solution, trypsin-EDTA, PBS, glutamine, LIVE/DEAD® Viability/Cytotoxicity Kit for mammalian cells and Qdot 800 streptavidin conjugate were supplied by Invitrogen. Restriction enzymes *Ear*I and *Hind*III, Alexa Fluor 488-labeled goat anti mouse secondary antibody (A21121) and EZ-Link Psoralen PEG_3 Biotin were purchased from ThermoFisher Scientific. SeaKem LE Agarose and DAPI were supplied by Lonza. Paraformaldehyde and Triton X-100 were purchased from Sigma.

2.2 Virus infections and titrations

The virulent South African RVFV strain 56/74 used in this study for mouse challenge studies has been described previously [35]. For titration of virus in post-challenge blood samples, serial ten-fold dilutions of blood-EDTA were mixed with freshly trypsinized Vero cells (duplicates) and seed on MW96 plates. Four days later, the cytopathic effect (cpe) was monitored and cells were fixed and stained with Crystal Violet stain. Titers are expressed as the log10 of the highest dilution where 50% of the wells showed cpe. The attenuated RVFV-MP12 strain [36] was used for seroneutralization studies.

2.3 Site-targeted mutagenesis

The plasmid pCMVNSmGn containing the RVFV-MP12 NSm/Gn sequence spanning nucleotides 21-2070 (GenBank accession number DQ380208) under transcriptional control of the human cytomegalovirus immediate early promoter (hCMVie) was mutated using QuickChange Site-Directed Mutagenesis Kit according to manufacturer's instructions. Briefly, the plasmid was incubated with two complementary oligonucleotides containing the desired mutation (Table 1), flanked by unmodified nucleotide sequence, and the reaction was performed by *Pfu* Turbo polymerase following manufacturer's instructions.

Primer	Sequence (5'-3')	Tm
MutSappCMVFor	GCGTATTGGGCGCTATTCCGCTTCCTCGAC	78.5°C
MutSappCMVRev	GTCGAGGAAGCGGAATAGCGCCCAATACGC	78.5°C
MutCterGnFor	GCCCCTATTCCTCGTCATGTATGAAGAGCTAGGCGGCCG	80.18°C
MutCterGnRev	CGGCCGCCTAGCTCTTCATACATGACGAGGAATAGGGGC	80.18°C

Table 1. Sequences of mutagenesis primers used for DNA mutagenesis.

After the reaction, the PCR products were incubated with restriction enzyme *Dpn*I for 1 hour at 37°C in order to digest parental DNA. Then, XL-1 Blue competent bacteria were transformed with PCR products, according to manufacturer's instructions. Briefly, 1 μL of the *Dpn*I treated DNA was transferred to a 50-μL aliquot of the competent cells. The transformation reactions were incubated on ice for 30 minutes and a heat pulse the 45 seconds at 42°C was performed. After 2 minutes on ice, 450 μL of preheated to 42°C SOC Medium were added and the transformation reactions were incubated at 37°C for 1 hour with shaking at 250 rpm. 100 μL of each transformation reaction was plated on agar plates containing ampicillin. The transformation plates were incubated at 37°C for 16 hours. Bacterial DNA was isolated and purified by using Endo Free Plasmid Maxi kit according to manufacturer's instructions. After DNA extraction, pure plasmids were incubated with restriction enzyme *Ear*I for 15 minutes at 37°C following manufacturer's instructions and visualized in agarose electrophoresis to check the purity of the plasmids. Results were corroborated by DNA sequencing.

2.4 Plasmid cloning, extraction and purification

The elastin-like recombinamers (ELRs) used in this work were obtained as described elsewhere [4]. The final fusion genes with a fully controlled composition and chain length were constructed by sequential introduction of the monomer gene segments in a stepwise manner using the recursive directional ligation method (RDL). Briefly, the mutated pCMVNSmGn plasmid was linearized by digestion with the restriction enzyme *Sap*I overnight at 37°C and corroborated by visualization in 1% agarose electrophoresis. The cloning of the linearized plasmid and corresponding ELR insert was performed by incubating with T4 DNA ligase for 1 hour at 22°C and used to transform competent bacteria XL-1 Blue according to manufacturer's instructions. Plasmid DNA was isolated and purified by using Endo Free Plasmid Maxi kit as above. After DNA

extraction, pure recombinant plasmids were analyzed by digestion with restriction enzyme *Hind*III for 15 minutes at 37°C following manufacturer's instructions and visualized in agarose electrophoresis. The gene sequence of every cloning step was corroborated by DNA sequencing. Endotoxin levels of the final gene constructs were determined using the Endosafe-PTSTM test (Charles River).

2.5 Cell culture

293T human embryonic kidney cells and African green monkey Vero cells were maintained in a humid atmosphere of 5% CO2 and 37°C in Dulbecco's modified Eagle's medium (DMEM)supplemented with 10% FBS, 2 mM glutamine, 100 U/mL penicillin and 0.1 mg/mL streptomycin. When required, cells were detached using a solution of 0.05% Trypsin-EDTA. BHK-21 (C-13) hamster kidney fibroblasts were cultured in EMEM Eagle's Minimum Essential Medium supplemented with 10% FBS, 100 U/mL penicillin and 0.1 mg/mL streptomycin at 5% CO_2 and 37 °C. When required, cells were collected using a solution of 0.05% Trypsin-EDTA.

2.6 Cell transfection

293T cells were seeded (2 x 10^4 cells per cm^2) and allowed to growth overnight. Then, transfection reagents Lipofectamine and Turbofect were prepared according to manufacturer's instructions for 20 minutes at room temperature. Transfection reagent/DNA mixture was added to cells. Cell medium was replaced by fresh medium after 24 hours and transgene expression was analyzed after 24 hours.

2.7 Cell viability assay

293T cells were transfected with plasmids as described above, and cytotoxic effect of the constructs was determined after 24 hours. Thus, LIVE/DEAD Viability/Cytoxicity Assay Kit was used according to the manufacturer's instructions. Briefly, a stock

solution of the LIVE/DEAD reagents (1 μM calcein AM and 2 μM EthD-1 in 10 mL of DPBS) was prepared and 100 μL were distributed in each well. After incubation for 20 minutes in the dark, the fluorescence intensity emission was measured at 525 and 645 nm after excitation at 485 and 525 nm (SpectraMax M5e Molecular Devices microplate reader). Additionally, photographic images of cultures were taken using a Nikon eclipse Ti-SR (Japan) fluorescence microscope. Three independent experiments, each in triplicate, were performed.

2.8 Gn expression immunodetection

293T cells were seeded (2.5 x 10^4 cells per well) and allowed to growth overnight in complete medium. After 24 hours, cells were transfected as described. 24 hours later, cells were washed with PBS 1X, fixed with PFA 4% and permeabilized with Triton X-100 0.1%. After washing with PBS 1X, cells were blocked by FBS 2% and incubated with RVFV-immunized mouse serum for 1 hour. Then, cells were washed with PBS 1X and incubated with Alexa Fluor 488-labeled secondary antibody and fluorescence intensity was measured by SpectraMax M5e Molecular Devices microplate reader. Three independent experiments, each in triplicate, were performed.

2.9 Confocal microscopy

293T cells were transfected with plasmids as explained above. After 24 hours, cells were washed with PBS 1X, fixed with PFA 4% and permeabilized with Triton X-100 0.1%. After washing with PBS 1X, cells were blocked by FBS 2% and incubated with RVFV-immunized mouse serum for 1 hour. Cells were then washed with PBS 1X three times and incubated with Alexa Fluor 488-labeled secondary antibody for 1 hour. Cells were washed with PBS 1X and cellular nuclei were stained with DAPI for 5 minutes.

Finally, cells were washed with PBS 1X. Confocal images were taken using a Leica TCS SP5 confocal microscope.

2.10 Immunization and challenge of mice

Groups of 12-16 week- old Balb/c mice were inoculated through the intramuscular (i.m) route with 100 µg of endotoxin free plasmid in saline with two doses at 2 weeks intervals. An additional booster plasmid dose was supplied 12 weeks later. Two weeks after the second boost and four weeks after the third dose (Figure 8A), animals were bled from the submandibular vein plexus. Sera post-vaccination were heat-inactivated at 56ºC for 30 minutes and kept at -20ºC until used. Four weeks after the last DNA dose, mice were challenged intraperitoneally (i.p) with 10^3 pfu of the RVFV isolate 56/74. Three days later, animals were euthanized, total EDTA-blood samples were collected and kept at -80º until use.

Mice were housed in a BSL-3 containment area with food and water supplied *ad libitum*. All experimental procedures were handled in accordance with EU guidelines from the 2010/63 EU Directive for animal experimentation, and protocols approved by INIA´s Committees for Biosafety and Ethics of Animal Experiments (permit codes CEEA 2012/014 and CBS 2012/017).

2.11 *In vivo* humoral immune responses

The presence of serum neutralizing antibodies was analyzed by plaque reduction neutralization assay. Briefly, a fixed amount of virus (100 pfu of the MP12 strain of RVFV) was incubated for 30 minutes at 37ºC with three-fold serum dilutions or with medium only. The mixture was then added onto Vero cells grown in 6-well plates. After 1 hour of adsorption, the inoculum was removed, cells were washed and a semi-

solid medium containing 1% Carboxy-methylcellulose (CMC, Sigma) was added. Monolayers were fixed and stained 3-5 days post infection. Cell lysis plaques were counted and the percentage of infectivity reduction for each serum dilution was calculated and expressed as $PRNT_{80}$. i.e, the dilution of serum (log10) rendering a reduction of infectivity of 80%.

2.12 *In vivo* cellular immune response assays

Spleen cells were obtained from grinded mouse spleens. Red blood cells were lysed by adding 0.16M NH_4Cl, washed with DMEM, and resuspended in DMEM supplemented with 10% FBS, 20 mM HEPES, 0.05 mM β-mercaptoethanol. For *in vitro* re-stimulation of lymphocytes, we followed two approaches: firstly, the spleen cells (10^6 cells/ml) were incubated with 5ug/ml of either a RVFV-Gn specific H2-K^d class-I MHC peptide (SYAHHRTLL), or medium alone with no stimulus. Secondly, 10^5 cultured cells from the murine macrophage cell line RAW 264.7 (ATCC- TIB-7) were infected in 96-well plates with RVFV 56/74 at a multiplicity of infection of 2. As a negative control, uninfected RAW 264.7 cells were used. 24 hours later, $5x10^5$ spleen cells were added to each well and the co-cultures were incubated four additional days. Supernatants were harvested and frozen at -80ºC until used.

2.13 Cytokine quantification by Luminex

Measurement of cytokine release by splenocytes was performed using a cytokine detection kit (Th1/Th2 Cytokine 11-Plex Mouse ProcartaPlex™ Panel). Briefly, the supernatants from re-stimulated cells (see above) were diluted 1:2 in medium and incubated with paramagnetic-fluorescent beads coated with 11 different anti-mouse cytokine antibodies. Biotin-labeled antibody was incubated and a streptavidin-phycoerithine (SAPE) was used as detector of the immune complexes. Fluorescence

was read using the MagPix xMAP 50 apparatus (Merck). Cytokine concentrations were estimated by interpolation of a curve fit generated by serially diluted cytokine standards using specific software (xPonent).

2.14 Statistical analysis

For *in vitro* Gn detection assays, data are reported as mean ± SD (n = 3). Statistical analysis involved an ANOVA test with subsequent Bonferroni method. *$p < 0.01$, **$p < 0.001$. For *in vivo* assays, statistical analysis involved a variance analysis (ANOVA) in combination with a subsequent test using the Bonferroni method for comparison of the means. For comparison of medians, the Kruskall-Wallis test was used instead. A p values of less than 0.05 were considered to be statistically significant. Data were handled using the SPSS Statistics software version 20 (IBM) and the GraphPad 6.0 software (Prism).

3. Results and Discussion

3.1 Plasmid design and synthesis

ELR biomaterials have been proposed for multiple biomedical applications, such as drug delivery or tissue engineering [2,9]. García-Arévalo *et al*. developed immunomodulatory nanocarriers as tuberculosis vaccines. These nanovaccines consisted on an amphiphilic ELR backbone decorated with the major membrane protein sequence from *Mycobacterium tuberculosis* [10]. Therefore, we hypothesized that ELR could be an accurate approach in order to improve viral Gn glycoprotein production in eukaryotic cells and/or to enhance its immunogenicity in mice. To that aim, we designed six constructs consisting on ELR gene blocks of different nature. The structure of the six fusion genes is depicted in Figure 1. Due to the hydrophilic nature of Gn glycoprotein, three different fusion genes (Gn-A80, Gn-I80 and Gn-V84) based on

hydrophobic residues, whose sequences were $(VPGAG)_{80}$, $(VGIPG)_{80}$ and $(VPGVG)_{84}$ respectively, were synthesized. Thus, amphiphilic structures could be built as a first approach. The second strategy consisted on one fusion gene (Gn-E75) based on hydrophilic glutamic acid, whose sequence was $[(VPGVG)_2\text{-}(VPGEG)\text{-}(VPGVG)_2]_{15}$. This construct could stay soluble without aggregation ability, due to the fact that glutamic acid is not able to self-assemble in a physiological environment [37-38]. Thus, we could compare the viral glycoprotein expression and immunogenicity between amphiphilic aggregates and soluble Gn-E75 construct. Moreover, we developed a new construct with two valine-rich blocks (Gn-V168) as third approach. Thus, the reinforced polymeric component could allow an easier aggregation under physiological conditions.

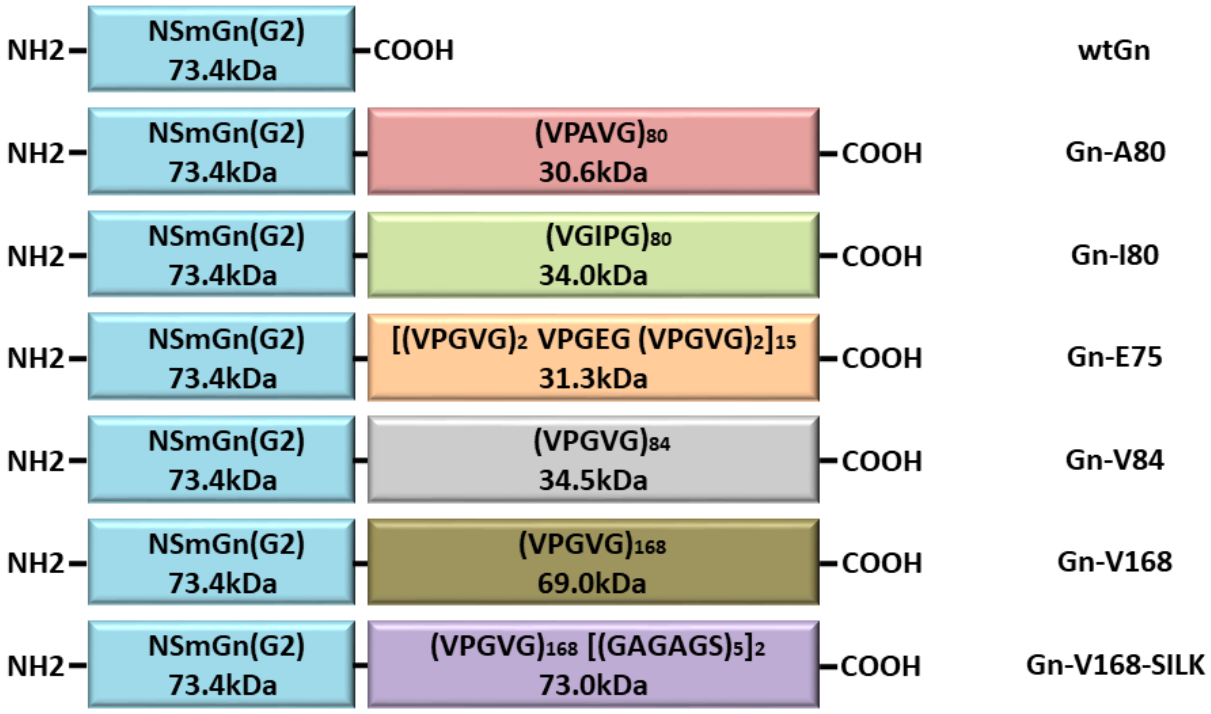

Figure 1. Design, composition and molecular weight of the developed fusion proteins. The ELR blocks include their amino acid composition. Non-scaled scheme.

Finally, the fourth strategy consisted on $[V(GAGAGS)_5G]_2$ sequence from silk fibroin produced by silkworm, which was added to Gn-V168 construct in order to improve the

aggregation stability (Figure 1). The silk fibroin produced by silkworm is characterized by its self-assembling ability into a highly stable amphiphilic β-sheet secondary structure [39-40].

3.2 Site-targeted mutagenesis

Site-targeted mutagenesis was performed in order to build the different constructs previously described. For this reason, a pCMV plasmid containing the gene codifying for glycoprotein Gn was mutated in order to allow us to add genes codifying for different ELRs constructs. This process was done in two steps (Figure 2).

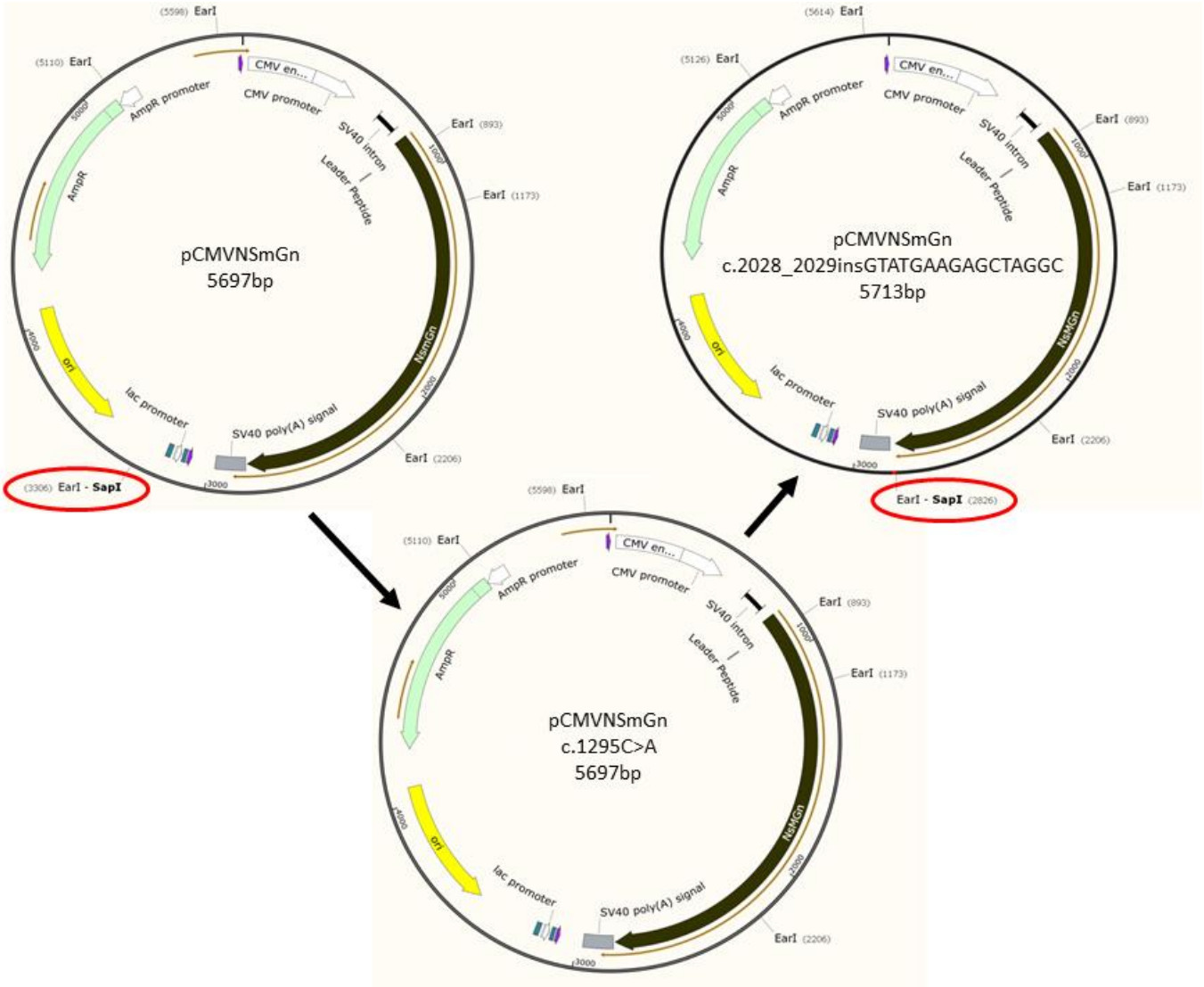

Figure 2. Composition of original and mutated plasmids. The recognition sites for restriction enzymes (*Ear*I and *Sap*I) and other features are indicated in the map.

First, an *Ear*I/*Sap*I recognition site (5'-GCTCTTC-3') was removed by the substitution of a cytosine for an adenine at position 3306 in the plasmid sequence (Table S1, Figures 2 and S1A). Two different mutagenesis primers were specifically synthesized and used for this site-directed mutagenesis (Table 1). Pure plasmidic DNA was incubated with restriction enzyme *Ear*I and visualized in agarose electrophoresis to check the success of the mutagenesis (Figure S1B). The theoretical fragments for the original plasmid (pCMV-NSmGn) were 280 bp, 488 bp, 992 bp, 1033 bp, 1100 bp and 1804 bp. On the other hand, the theoretical fragments for the mutated plasmid were 280 bp, 488 bp, 992 bp, 1033 bp, 2904 bp. Due to the mutation c.1295C>A, an *Ear*I/*Sap*I recognition site was removed from position 3306 (Figure 2) and, as a consequence, the fragments of 1100 and 1804 bp were fused in one fragment of 2904 bp length. Results were corroborated by DNA sequencing.

Once the deletion of this *Sap*I recognition site was performed and checked (Figure S1), a second site-directed mutagenesis was performed in order to introduce a new *Sap*I recognition site (5'-GAAGAGC-3') after Gn glycoprotein codifying gene. Thus, genes codifying for different ELRs could be introduced next to the viral glycoprotein Gn gene and achieve the final fusion genes (Figure S2-S8). For this purpose, two mutagenesis primers were specifically synthesized (Table 1). This second mutation consisted on the insertion of the 16 nucleotides "GTATGAAGAGCTAGGC" at position 2826 in the plasmid sequence. As described above, the introduction of this new *Sap*I recognition site was corroborated by *Ear*I digestion (Figure S1) and DNA sequencing. The theoretical fragments for the final plasmid were: 280 bp, 488 bp, 620 bp, 992 bp, 1033 bp and 2300 bp. Due to the mutation c.2028_2029insGTATGAAGAGCTAGGC, an

*Ear*I/*Sap*I recognition site was created at position 2826. As a consequence, the fragment of 2904 bp length was split in two fragments of 620 and 2300 bp, respectively. Thus, after the second mutation, the pCMVNSmGn plasmid was already prepared for introducing ELR genes from a gene library in order to develop different constructs which could improve the expression of viral glycoprotein Gn in eukaryotic systems.

3.3 Construct synthesis

Briefly, the doubly mutated pCMVNSmGn plasmid (hereafter termed wtGn) was linearized by digestion with the restriction enzyme *Sap*I and the corresponding ELR insert cloned in the vector. Competent bacteria were transformed with ligation mixture and selected by Ampicillin resistance. After plasmidic DNA isolation and purification, recombinant plasmids were identified by diagnostic *Hind*III digestion. As can be seen in Figures S2-S8, all the constructs showed fragments of the expected length. These results confirmed the accurate synthesis of the constructs. Furthermore, the sequences were corroborated by DNA sequencing. Endotoxin levels were measured and were lower than 0.25 EU/mg in all cases.

3.4 Analysis of cell viability upon DNA transfection

One of the aims of this work was to obtain recombinant constructs able to improve the expression level of viral glycoprotein Gn in eukaryotic cells. Therefore, these plasmid constructs should be completely innocuous upon cell uptake. Cell viability was determined after transfection of the plasmid constructs in order to assess the suitability of the plasmid constructs (Figures 3 and S9). In order to transfect 293T cells, either Lipofectamine or Turbofect transfection systems were used, as both are some of the most standard transfection systems.

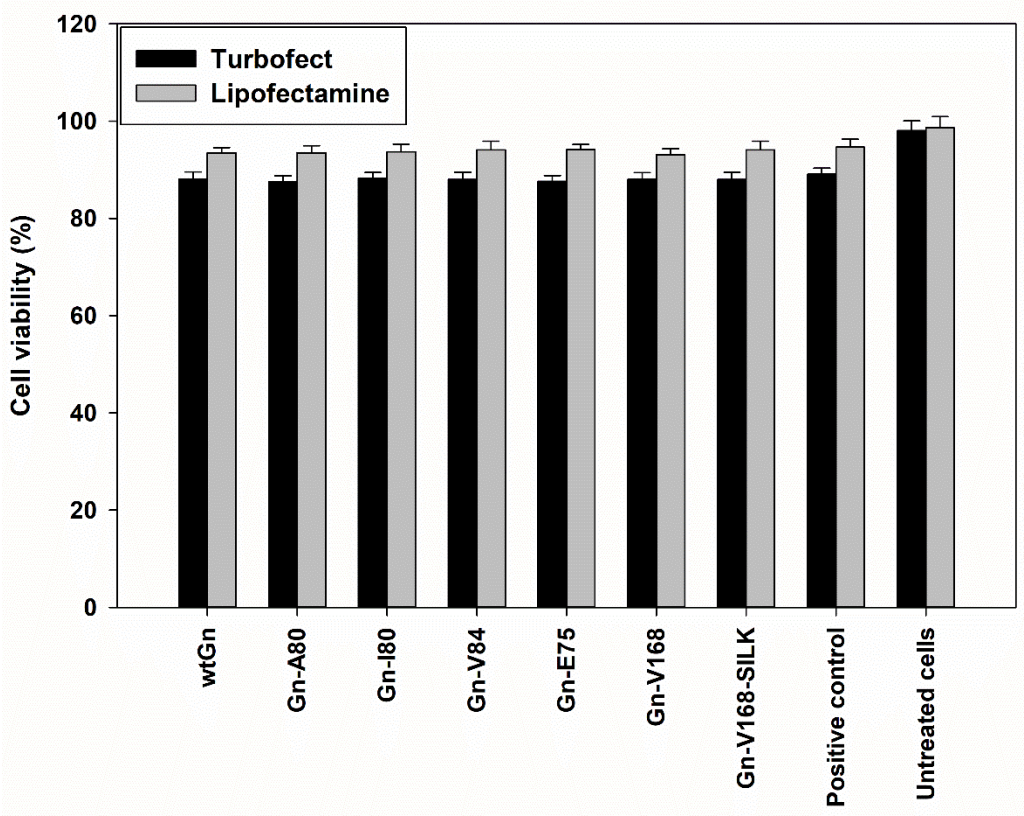

Figure 3. Percentage viability of 293T human embryonic kidney cells. after transfection of DNA constructs with Lipofectamine or Turbofect. Cells were transfected with corresponding DNA construct and viability was measured 24 hours later using the LIVE/DEAD assay kit. n = 3 independent experiments, mean ± SD.

Transfected cells with different fusion genes showed similar viability levels to transfected cells with control plasmid. At light of this result, we could conclude that the slightly effect on cell viability was due to the transfection procedure and none of the different gene constructs seemed to significantly affect cell viability. Thus, these results highlighted that the developed plasmid constructs were safe, one of the requirements when working with DNA vaccines. Moreover, cell viability was higher in Lipofectamine treated cells compared to Turbofect ones (Figures 3 and S9). For this reason, we used Lipofectamine as transfection reagent in the following experiments.

3.5 Analysis of Gn glycoprotein detection

Once the gene constructs were shown innocuous, the expression of Gn glycoprotein in eukaryotic cells was determined in order to compare the production levels of the fused genes with respect to the expression of the non-fused Gn viral antigen (Figure 4). For this purpose, 293T cells were transfected as explained above and Gn glycoprotein expression was measured by immunocytochemistry. Hyperimmune serum from RVFV-infected mice was used as primary antibody. The pCMV-DM plasmid containing the gene codifying for RVFV Gn glycoprotein was used as positive control. As can be seen in Figure 4, for both Gn-A80 and Gn-I80 the expression levels were lower than those of the positive control. However, either Gn-E75 or Gn-V84 constructs significantly increased the detection of RVFV Gn glycoprotein (40% and 29%, respectively). Interestingly, Gn-V84 showed higher Gn expression levels, contrarily to the results shown by the other amphiphilic constructs Gn-A80 and Gn-I80. The enhanced detection of Gn glycoprotein comprised in the Gn-E75 construct correlated to the fact that the viral antigen was soluble instead of assembled in amphiphilic aggregates. Moreover, both the Gn-V168 and Gn-V168-SILK construct, containing two blocks of Valine and gene codifying for worm silk, showed similar Gn glycoprotein expression levels than the positive control. Even though the viral glycoprotein expression level in transfected cells with the Gn-V168 construct was higher than the level shown by cells transfected with positive control, this difference was not statistically significant.

These results, in which longer constructs did not improve Gn expression, could be due to the fact that large proteins are difficult to be translated and processed in eukaryotic cells. Furthermore, an excessive hydrophobicity of these constructs could difficult their translation in eukaryotic cells. Thus, we could conclude that the expression of Gn

glycoprotein was not improved by constructs with hydrophobic ELR blocks, as Isoleucine and Alanine. Contrarily, less hydrophobic Gn-V84 and hydrophilic Gn-E75 constructs significantly improved the antigen expression in 293T cells. Thus, we could conclude that our constructs would be a promising approach in order to produce huge amounts of antigens *in vitro.* This system could be used as an accurate strategy to improve the production of natural antigens needed for vaccines involving a scaled up process and reduced productions costs. As a consequence of these results, Gn-E75, Gn-V84, Gn-V168 and Gn-V168-SILK encoding plasmid constructs were chosen for the *in vivo* assays in order to determine their ability to induce anti-Gn immune responses in mice.

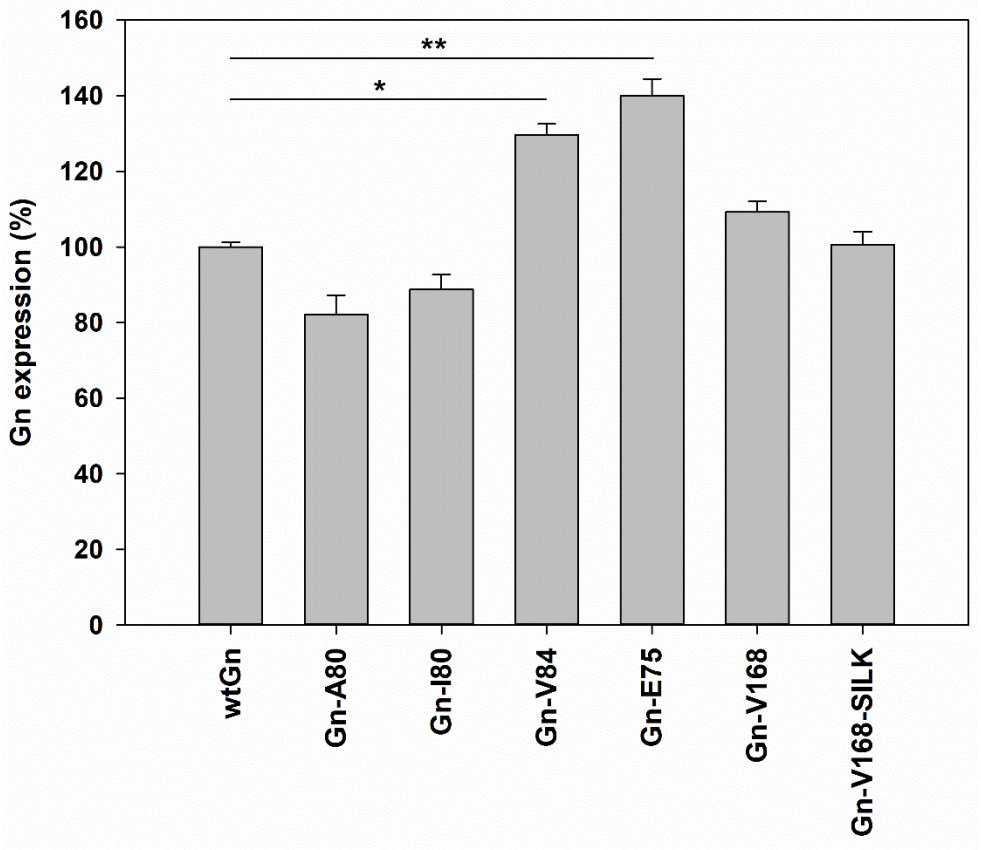

Figure 4. Detection levels of Gn glycoprotein in 293T human embryonic kidney cells. Cells were transfected with Lipofectamine and the indicated DNA construct. After 24 hours, cells were fixed, permeabilized and blocked. After incubation with RVFV-

immunized mouse serum and secondary antibody, fluorescence intensity was measured in a plate reader. Three independent experiments were performed. Bars denote mean ± SD. *p < 0.01; **p < 0.001.

Furthermore, confocal fluorescence images were taken in order to determine cellular localization of translated fusion proteins after cell transfection with gene constructs. As it can be seen in Figures 5 and 6, fusion protein composed by ELRs and viral Gn glycoprotein showed cytoplasmic localization in all cases. This result suggests that the presence of ELR blocks did not change the perinuclear localization of the fusion proteins, regardless of its amino acid composition. Indeed, there were no differences in cellular localization between those constructs that improved Gn expression and those provoking lower expression levels.

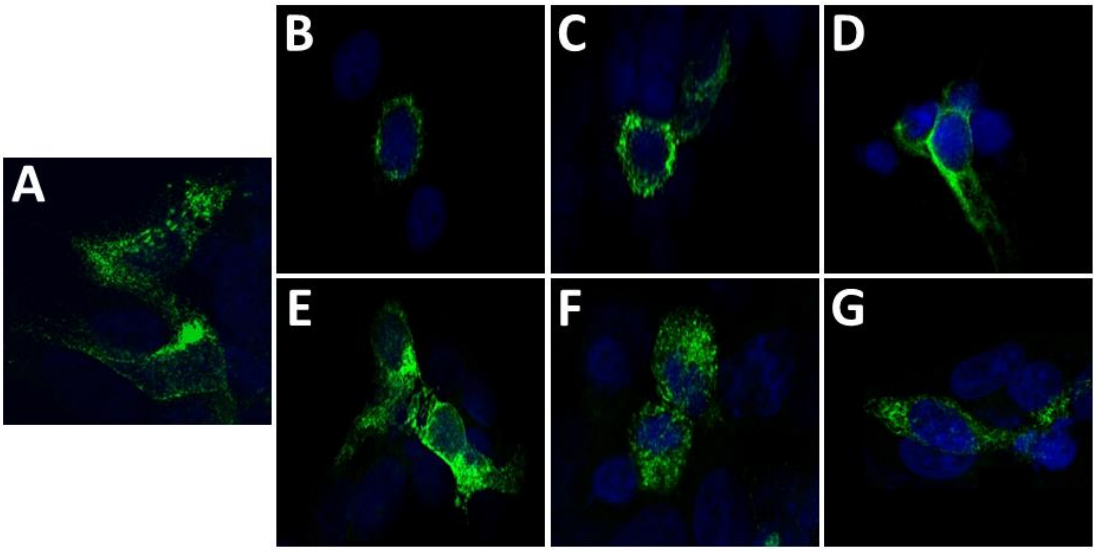

Figure 5. Confocal microscopy images of 293T human embryonic kidney cells after transfection of DNA constructs with. Cells were transfected with Lipofectamine and the corresponding DNA construct. After 24 hours, cells were fixed with PFA 4%, permeabilized with Triton X-100 0.1 and blocked by FBS 2%. After incubation with

RVFV-immunized mouse serum, confocal pictures were taken. A: wtGn; B: Gn-A80; C: Gn-I80; D: Gn-V84; E: Gn-E75; F: Gn-V168; G: Gn-V168-SILK;

As expected, fusion constructs involving ELR blocks composed by hydrophobic amino acids (Gn-A80, Gn-I80, Gn-V84, Gn-V168 and Gn-V168-SILK) seemed to show an aggregation-like appearance (Figures 5 and 6). These microscopic aggregates could be due to amphiphilic structures, as a consequence of the hydrophilic nature of RVFV Gn glycoprotein. Thus, when the hydrophobic component was increased, aggregates were observed. In contrast, cells transfected with Gn-E75 construct showed higher viral glycoprotein expression in the whole cytoplasm without aggregation appearance. This could be due to the fact that glutamic acid remains soluble and is not able to self-assemble in an ordered structure [37-38].

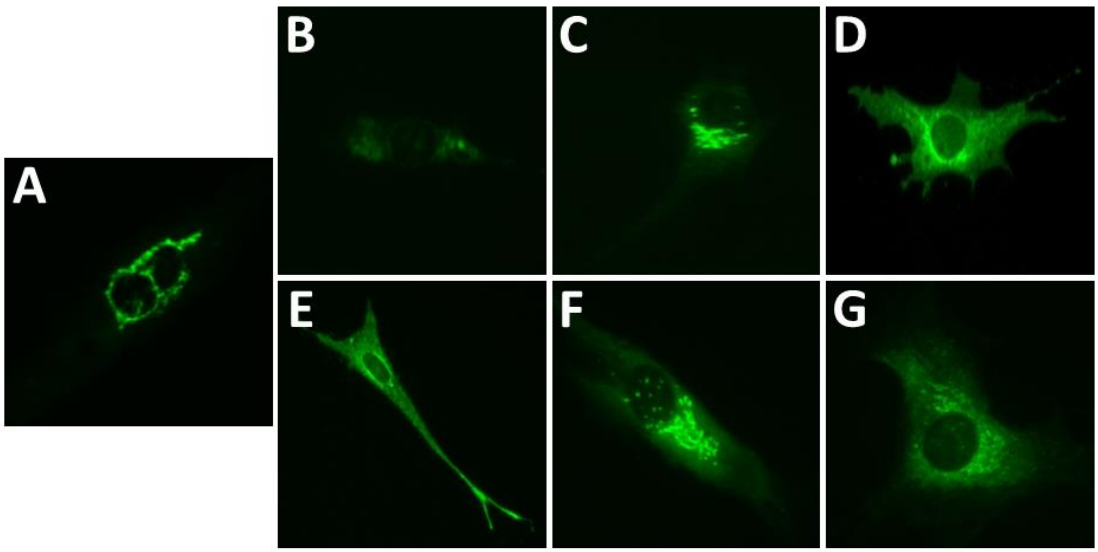

Figure 6. Confocal microscopy images of BHK-21 (C-13) hamster kidney fibroblasts after transfection of DNA constructs with. Cells were transfected with Lipofectamine and the corresponding DNA construct. After 24 hours, cells were fixed with PFA 4%, permeabilized and blocked. After incubation with RVFV-immunized mouse serum and

secondary antibody, confocal pictures were taken. A: wtGn; B: Gn-A80; C: Gn-I80; D: Gn-V84; E: Gn-E75; F: Gn-V168; G: Gn-V168-SILK;

3.5 Analysis of neutralizing antibody responses and efficacy elicited upon plasmid immunization in mice

Upon immunization, the development of a neutralizing antibody response was analyzed after two or three plasmid DNA intramuscular doses. In general, two plasmid doses were insufficient to achieve a robust and consistent neutralizing antibody response, with only few animals within each group developing detectable but low titers of antibodies (Figure 7, empty symbols). However, higher and statistically significant neutralizing responses were detected in 100% of the animals in the group receiving the plasmid expressing wtGn. After a third DNA boost neutralizing titers were clearly enhanced in all groups (Figure 7, full symbols), although a few animals remained negative in some groups (Gn-E75, Gn-V168-SILK and Gn-V168). No clear differences were observed in the group immunized with the Gn-V168-SILK construct and, surprisingly, the sera from wtGn group animals collected after the third plasmid dose showed a decrease in their neutralization titers. This could be due to the fact that expression levels of the viral antigen, when combined with ELR constructs, could have longer half-life compared to wild type antigen. Despite these single differences, statistical analysis did not reveal significant differences among mean values of neutralizing antibody titers obtained after 3 doses of the different DNA constructs assayed.

Three days after the last DNA booster dose, mice were subjected to virus challenge with a lethal dose of the virulent RVFV strain 56/74. A naïve (mock-immunized) group of mice was included as a control. At day 3 p.i., when viremia is known to reach a peak in infected animals, blood samples were collected and viral loads were analyzed. Results

are shown in Figure 8. All groups showed a clear reduction in viremia levels compared to the infected control group (mean value = 5.29 ±0.48). This decrease was around one log unit lower for the groups immunized with either Gn-E75 or Gn-V168-SILK constructs (mean values of 4.06 ±0.37 and 4.31 ±0.85, respectively; differences not statistically significant). In contrast groups receiving Gn-V84 or Gn-V168 plasmids showed reductions of 2 log units (mean values of 2.95 ±1.46 and 3.1 ±1.02, respectively. $p < 0.001$), and 40% of the animals rendering viral loads at or below the detection limit of the assay. As expected from the higher neutralizing titers reached during immunization, the group of mice immunized with the wtGn expressing construct showed lower or undetectable viremia levels (mean value = 1.80 ± 0.45; $p<0.0001$).

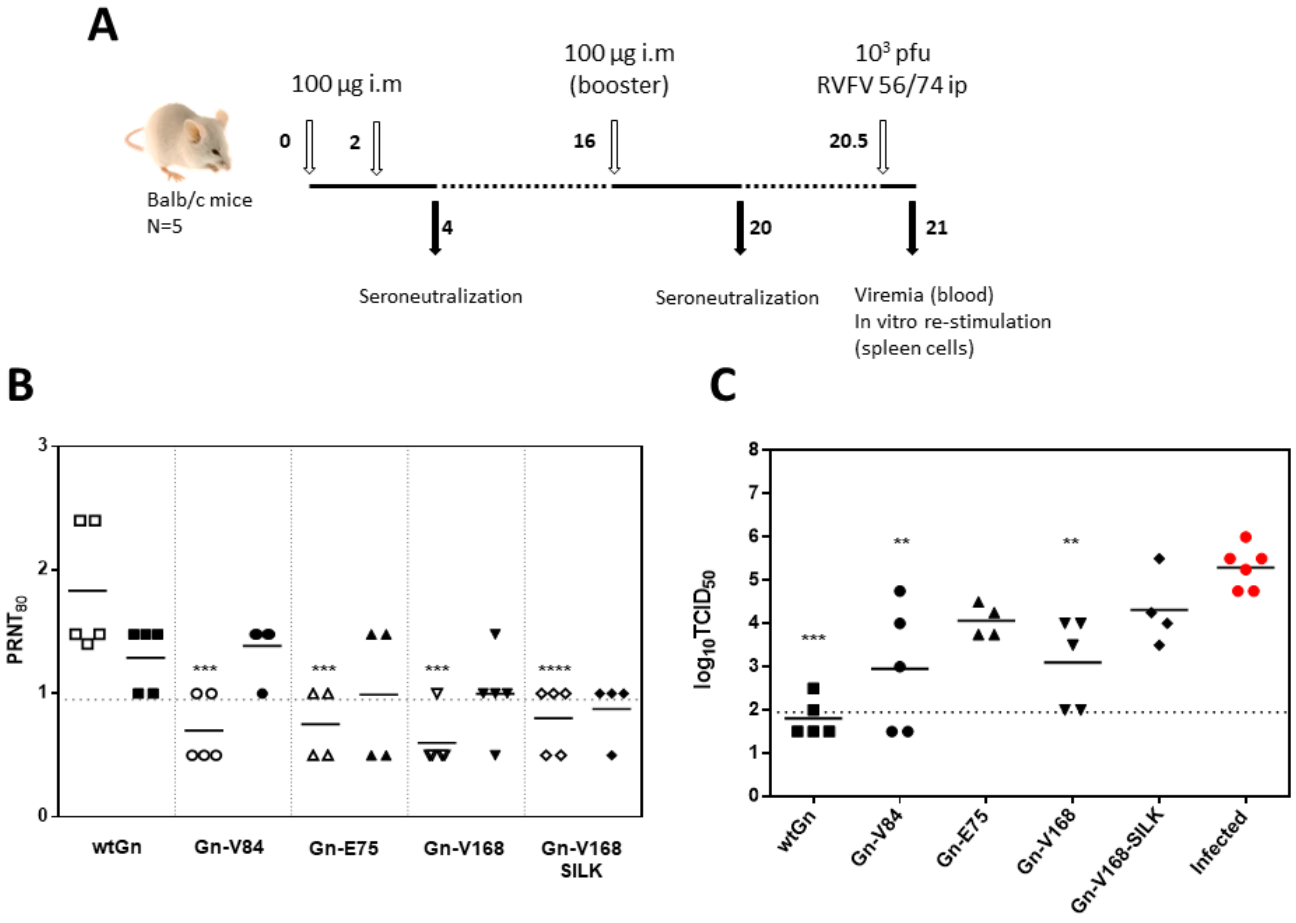

Figure 7. A: Scheme of the immunization and challenge of mice. BALB/c mice (n=5) were intramuscularly immunized twice with each plasmid construct with an additional boost 12 weeks later (open arrows). Mice were challenged intraperitoneally with 10^3 pfu of virulent RVFV 56/74. Blood samples were collected to monitor immune responses and viremia (closed arrows). Numbers indicate weeks after the starting of the experiment. B: Neutralizing antibodies after immunization. Titers of serum neutralizing antibodies after two (empty symbols) or three immunizations (closed symbols). Each symbol corresponds to a single mouse. Titers correspond to the mean dilutions of serum that reduce the number of plaques by 80% in a plaque reduction neutralization test (PRNT). Serum dilutions are expressed as $\log_{10}$. Horizontal dotted line depicts the sensitivity of the assay. Negative values were given an arbitrary value of 0.5 log. One way Anova with Bonferroni multiple comparisons was used for testing the statistical significance. *p* values are shown with respect to wtGn group (***p<0.001 ****p<0.0001). C. Viremia after challenge of immunized mice. 3 days after viral challenge the mice were euthanised and diluted blood samples tested on Vero cells for the presence of infectious virus. Each symbol corresponds to a single mouse. Group means are shown. Titers correspond to the mean dilutions of blood causing 50% of citopathic effect in vitro in a tissue culture infectivity dose (TCID) assay. Horizontal dotted line depicts the sensitivity of the assay. Negative values were given an arbitrary value of 1.5 log. One way Anova with Bonferroni multiple comparisons was used for testing the statistical significance. *p* values are shown with respect to infected (mock vaccinated) group (**p<0.01 ***p<0.001).

These results suggest that, even though variability between individual mice within the groups was high, the best responses in terms of reduction of viral load were achieved by

immunization with constructs Gn-V84 and Gn-V168, without correlation with the levels of Gn protein expression in cultured transfected cells (Figure 4). Thus, it is possible to assume that the quantity of Gn expression in vitro did not correlate with the neutralization levels nor efficacy in vivo, and that the immunogenicity of the constructs may be conditioned by other factors. Among these, the level of aggregation could benefit the magnitude and duration of the immune responses in terms of neutralization as suggested by the data from immunization with the more hydrophobic Gn-V84 or Gn-V168 constructs.

3.7 Analysis of the cellular immunity in mice upon viral challenge.

In order to gain more insight in the type of immune responses elicited by the different constructs, the induction of cellular immunity was assessed by in vitro re-stimulation of spleen cells obtained upon virus challenge. The measurement of the Th1/Th2 cytokine balance is a good indicative of the extent of antigen-specific cellular immune responses. A luminex-based assay was performed using supernatants of spleen cells collected after stimulation with either a class-I restricted Gn peptide described previously [41] or with virus infected antigen-presenting RAW 264.7 cells. This cell line retains characteristics of an antigen presenting cell (APC). Upon isolation, the viability of the spleen cells used for re-stimulation ranged between 80-95% (not shown). The re-stimulation with the Gn peptide increased the secretion of IFNγ in agreement with the class-I MHC restricted nature of the peptide. IFNγ levels were increased in wtGn, Gn-V84, Gn-V168 and Gn-V168SILK but not in non-vaccinated mice (mock) and Gn-E75 groups, although these differences did not reach statistical significance. Compared to mock treated cells, the stimulation of wt-Gn spleen cells showed significantly increased secretionsof IL12p70In turn, Gn-V168 induced a higher expression of IL1β, and IL12p70when compared to mock treated cells (Figure 8A). Interestingly, both wt-Gn

and Gn-V168 groups secreted significantly higher levels of IL-6 than the mock group, and Gn-V168 had also increased levels of IL4, IL5 and IL13 indicating a strong Th2 polarization (Figure 8B). Therefore, a more balanced T-cell response was promoted by the V168 construct.

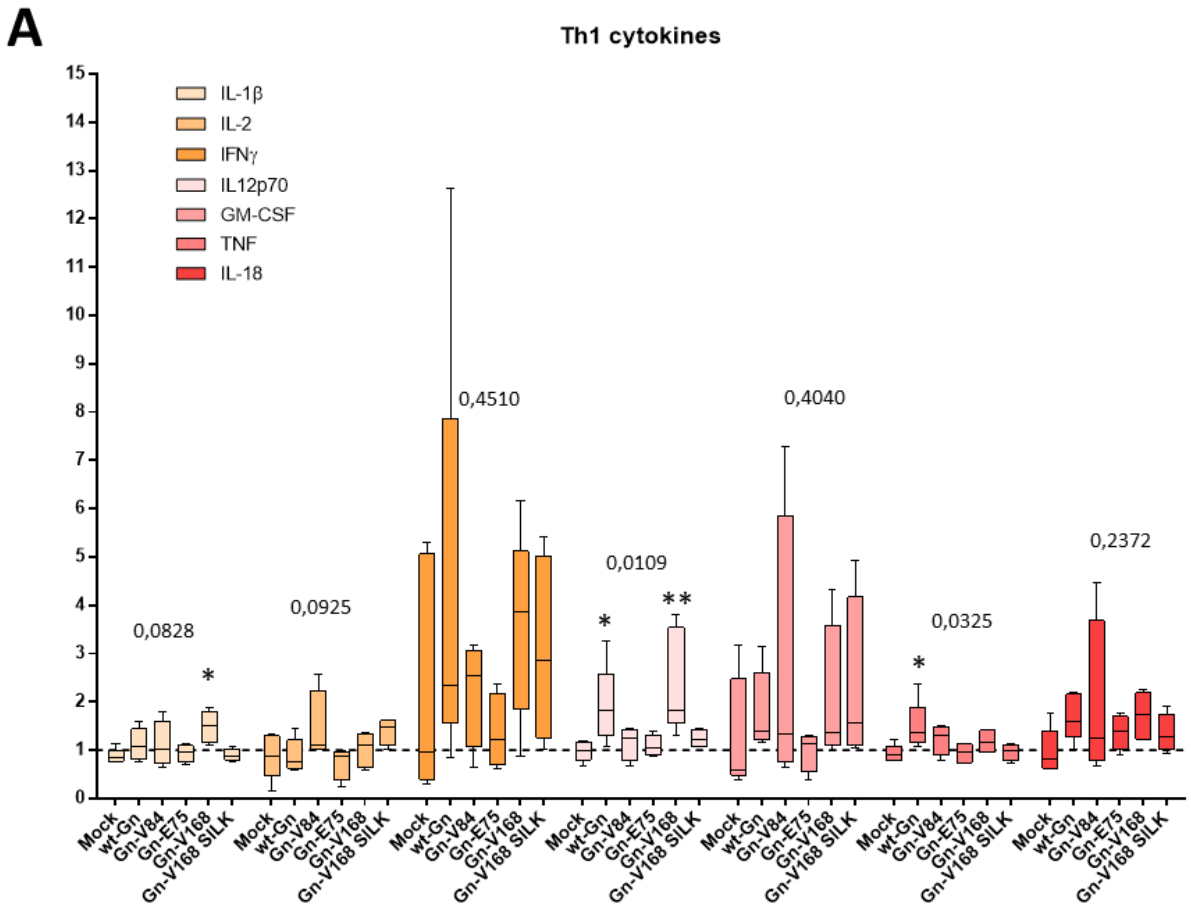

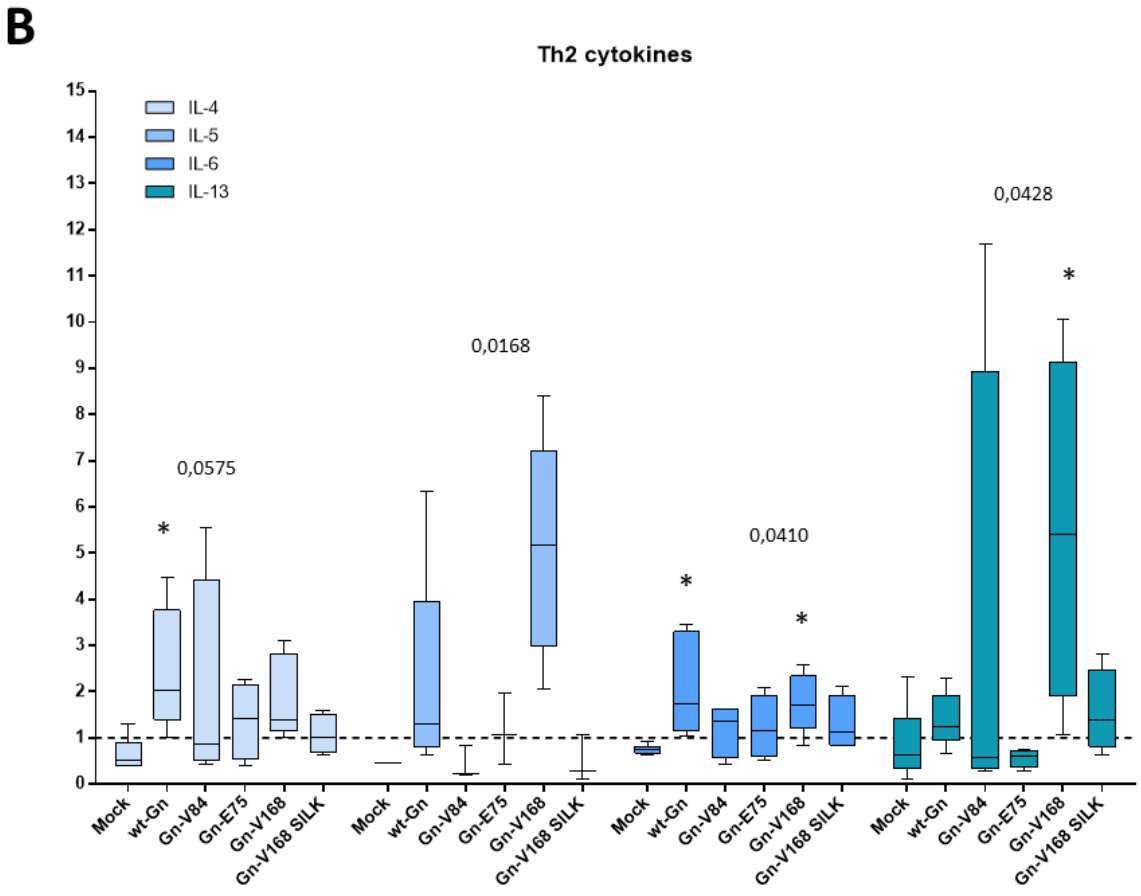

Figure 8. Th1 (A) or Th2 (B) cell associated cytokines secreted by cultured spleen cells upon stimulation with a Gn peptide. The values on the Y axis correspond to the stimulation index (ratio specific peptide/ medium). Each box represents the interquartile rank defined by the median value (horizontal line) for the indicated groups of immunized and 3-day infected mice. Mock group refers to the non-immunized and infected mice. Values above 1 (horizontal dotted line) indicate a positive stimulation. Numbers above bars indicate p values (Anova, non-parametric Kruskall-Wallis test). Asterisks indicate the level of significance with respect to the mock immunized group. *$p<0.05$, **$p<0.01$. IL-5 index values were not determined for the mock group due to the low sensitivity of the assay. Only three values were obtained for Gn-V84, Gn-E75 and Gn-V168 silk.

In contrast, the cytokine secretion elicited by infected RAW 264.7 cells was predominantly IFN-γ and IL-12, perhaps as a consequence of the activation of naive CD4 cells. The Gn-V168 and wt-Gn constructs induced the strongest bias towards Th2 responses in which IL-13 was more prominently secreted. These data indicate that, among the ELR plasmid constructs, Gn-V168 induced stronger levels of cell-mediated soluble effectors, perhaps contributing more efficiently to the protective phenotype observed after viral challenge.

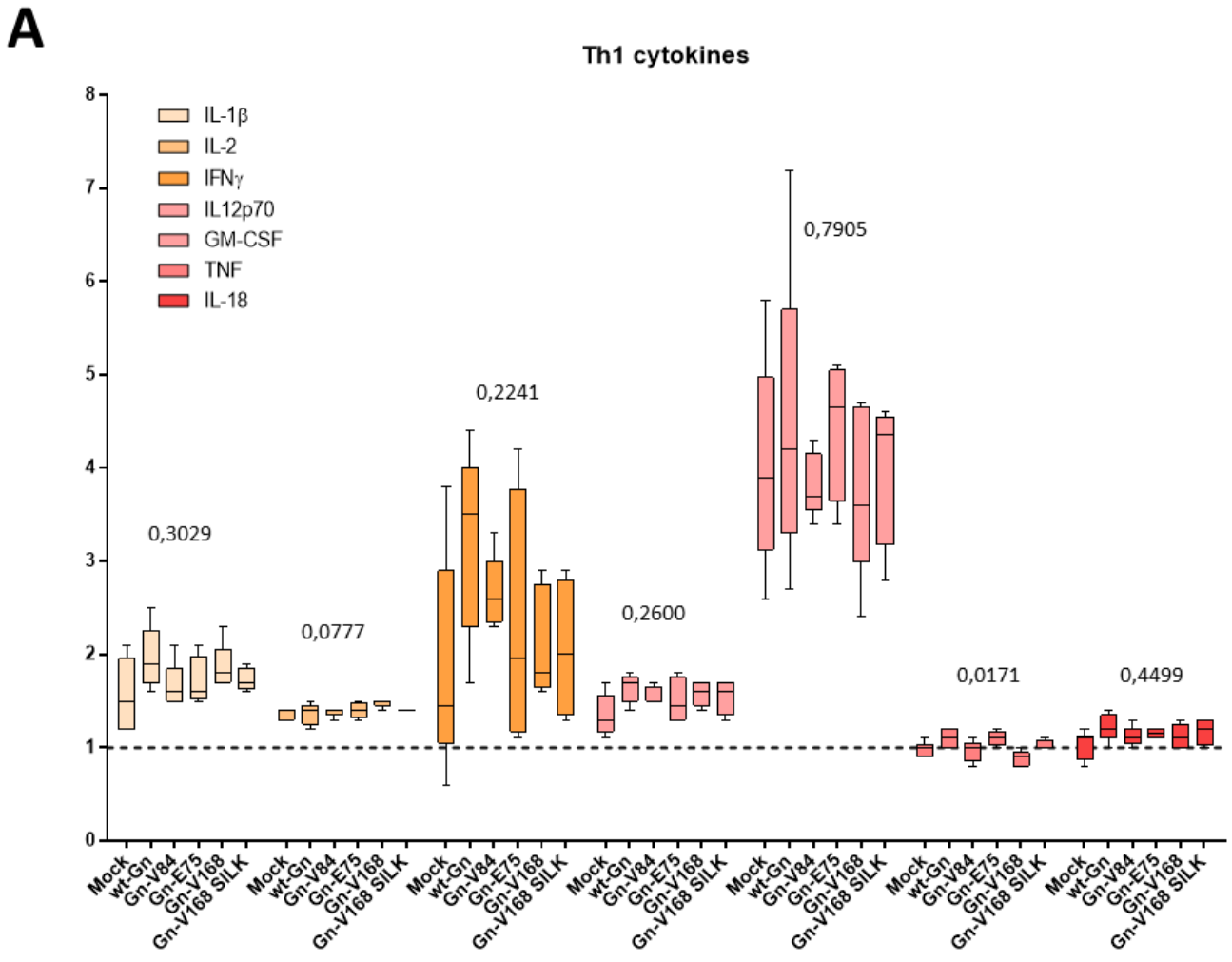

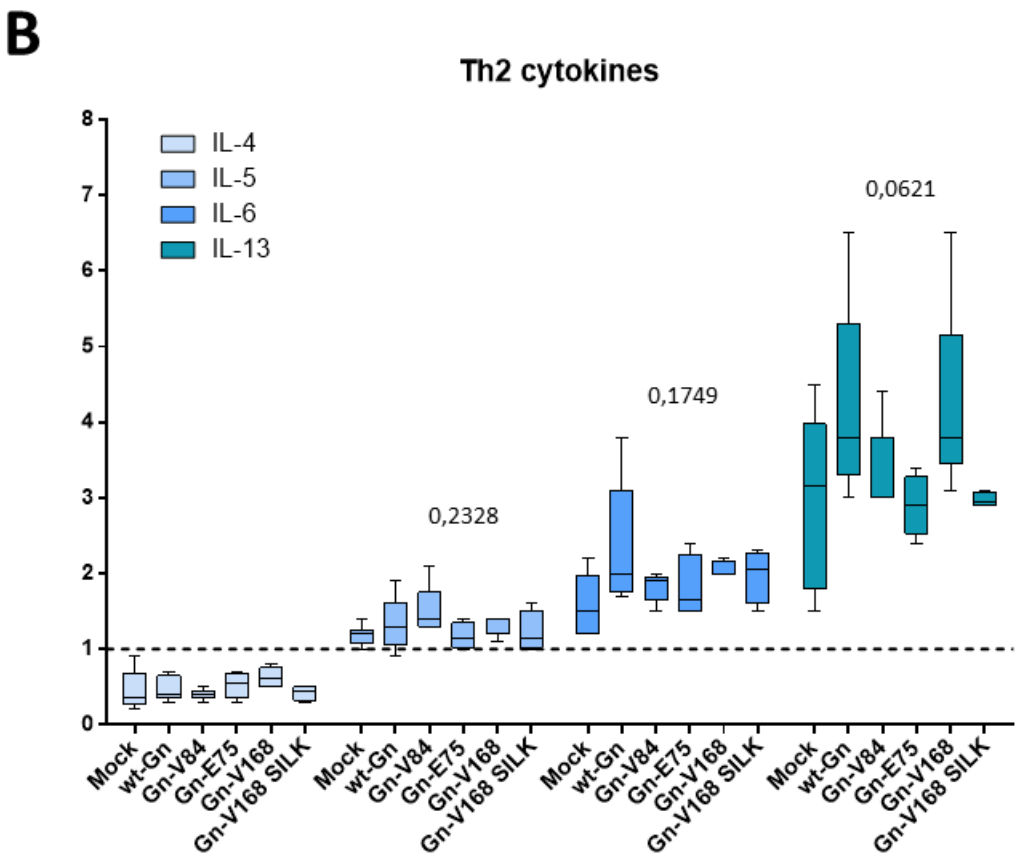

Figure 9. Th1 (A) or Th2 (B) cell associated cytokines secreted by cultured spleen cells upon stimulation with infected RAW 264.7 cells. The values on the Y axis correspond to the stimulation index (ratio infected cells/non-infected cells). Each box represent the interquartile rank defined by the meadian value (horizontal line) for the indicated groups of immunized and 3-day infected mice. Mock group refers to the non-immunized and infected mice. Values above 1 (horizontal dotted line) indicate a positive stimulation. Numbers above bars indicate p values (Anova non-parametric Kruskall-Wallis test).

4. Conclusions

In this work, we have developed novel ELR-based devices that are able to modulate the immunogenicity of Rift Valley fever virus glycoprotein Gn First, viability in eukaryotic cells was not affected after transfection with genetic plasmids, which showed that our constructs are safe, one of the most important requirements for DNA vaccination.

Moreover, two different constructs, Gn-E75 (with an ELR block based on glutamic acid) and Gn-V84 (whose ELR block contained valine), enhanced the viral glycoprotein expression. Therefore, this system could be a promising approach in order to achieve high yield productions of natural antigens, which could have great importance when huge amounts of vaccines are needed in pandemic situations or animal vaccinations. *In vivo* immune-challenge experiments in a mouse animal model determined the immunogenicity and efficacy after challenge of the construct Gn-V168. Thus, these constructs are highly suitable for further studies.

To the best of our knowledge, this study is the first work in which ELR-based biomaterials are used for the development of vaccines against RVFV. Biomaterials constitute a promising strategy for gene and drug delivery purposes and, for instance, ELR polyplexes could be an interesting approach for the development of accurate carriers of viral antigens in order to improve immunogenicity in eukaryotic systems. Nonetheless, further studies are needed to study these constructs in other *in vivo* models resembling the disease. Thus, patients developing RVF may be candidates for therapeutic treatment with ELR-based vaccines. Therefore, based on our findings, we can conclude that this novel approach could be a promising strategy for improving the immunogenicity of different antigens from multiple diseases in the future.

Conflict of interest

The authors declare no competing financial interest.

Acknowledgments

The authors are grateful for financial support from the European Social Fund (ESF) and the European Regional Development Fund (ERDF), as well as funding from the EU (NMP-2014-646075), the MICIUN (DTS19/00162, MAT2016-79435-R, MAT2016-78903-R and AGL2017-82336-R), the Comunidad de Madrid (project S2018/BAA-4370) the JCyL (project VA317P18), the CIBER-BBN, the JCyL and the Instituto de Salud Carlos III under the "Network Center of Regenerative Medicine and Cellular Therapy of Castilla and Leon".

References

1. Goldberg, M.; Langer, R.; Jia, X. Nanostructured materials for applications in drug delivery and tissue engineering. *J Biomater Sci Polym Ed.* **2007,** *18* (3), 241-68.
2. MacEwan, S. R.; Chilkoti, A. Applications of elastin-like polypeptides in drug delivery. *J Control Release.* **2014,** *190*, 314-30.
3. Girotti, A.; Fernandez-Colino, A.; Lopez, I. M.; Rodriguez-Cabello, J. C.; Arias, F. J. Elastin-like recombinamers: biosynthetic strategies and biotechnological applications. *Biotechnol J.* **2011,** *6* (10), 1174-86.
4. Rodriguez-Cabello, J. C.; Girotti, A.; Ribeiro, A.; Arias, F. J. Synthesis of genetically engineered protein polymers (recombinamers) as an example of advanced self-assembled smart materials. *Methods Mol Biol.* **2012,** *811*, 17-38.
5. Rodriguez-Cabello, J. C.; Arias, F. J.; Rodrigo, M. A.; Girotti, A. Elastin-like polypeptides in drug delivery. *Adv Drug Deliv Rev.* **2016,** *97*, 85-100.
6. Pina, M. J.; Girotti, A.; Santos, M.; Rodriguez-Cabello, J. C.; Arias, F. J. Biocompatible ELR-Based Polyplexes Coated with MUC1 Specific Aptamers and Targeted for Breast Cancer Gene Therapy. *Mol Pharm.* **2016,** *13* (3), 795-808.
7. Gonzalez-Valdivieso, J.; Girotti, A.; Munoz, R.; Rodriguez-Cabello, J. C.; Arias, F. J. Self-Assembling ELR-Based Nanoparticles as Smart Drug-Delivery Systems Modulating Cellular Growth via Akt. *Biomacromolecules.* **2019,** *20* (5), 1996-2007.
8. Pina, M. J.; Alex, S. M.; Arias, F. J.; Santos, M.; Rodriguez-Cabello, J. C.; Ramesan, R. M.; Sharma, C. P. Elastin-like recombinamers with acquired functionalities for gene-delivery applications. *J Biomed Mater Res A.* **2015,** *103* (10), 3166-78.
9. Santos, M.; Serrano-Ducar, S.; Gonzalez-Valdivieso, J.; Vallejo, R.; Girotti, A.; Cuadrado, P.; Arias, F. J. Genetically Engineered Elastin-based Biomaterials for Biomedical Applications. *Curr Med Chem.* **2018**.
10. Garcia-Arevalo, C.; Bermejo-Martin, J. F.; Rico, L.; Iglesias, V.; Martin, L.; Rodriguez-Cabello, J. C.; Arias, F. J. Immunomodulatory nanoparticles from elastin-like recombinamers: single-molecules for tuberculosis vaccine development. *Mol Pharm.* **2013,** *10* (2), 586-97.
11. Pisal, D. S.; Kosloski, M. P.; Balu-Iyer, S. V. Delivery of therapeutic proteins. *J Pharm Sci.* **2010,** *99* (6), 2557-75.
12. Ulmer, J. B.; Donnelly, J. J.; Parker, S. E.; Rhodes, G. H.; Felgner, P. L.; Dwarki, V. J.; Gromkowski, S. H.; Deck, R. R.; DeWitt, C. M.; Friedman, A.; et al. Heterologous protection against influenza by injection of DNA encoding a viral protein. *Science.* **1993,** *259* (5102), 1745-9.

13. Donnelly, J. J.; Wahren, B.; Liu, M. A. DNA vaccines: progress and challenges. *J Immunol.* **2005,** *175* (2), 633-9.
14. Kutzler, M. A.; Weiner, D. B. DNA vaccines: ready for prime time? *Nat Rev Genet.* **2008,** *9* (10), 776-88.
15. Brun, A. Vaccines and Vaccination for Veterinary Viral Diseases: A General Overview. *Methods Mol Biol.* **2016,** *1349*, 1-24.
16. Bouloy, M.; Flick, R. Reverse genetics technology for Rift Valley fever virus: current and future applications for the development of therapeutics and vaccines. *Antiviral Res.* **2009,** *84* (2), 101-18.
17. Dal Pozzo, F.; Thiry, E. Antiviral chemotherapy in veterinary medicine: current applications and perspectives. *Rev Sci Tech.* **2014,** *33* (3), 791-801.
18. Paweska, J. T. Rift Valley fever. *Rev Sci Tech.* **2015,** *34* (2), 375-89.
19. Borrego, B.; de Avila, A. I.; Domingo, E.; Brun, A. Lethal Mutagenesis of Rift Valley Fever Virus Induced by Favipiravir. *Antimicrob Agents Chemother.* **2019,** *63* (8).
20. Linthicum, K. J.; Britch, S. C.; Anyamba, A. Rift Valley Fever: An Emerging Mosquito-Borne Disease. *Annu Rev Entomol.* **2016,** *61*, 395-415.
21. Pepin, M.; Bouloy, M.; Bird, B. H.; Kemp, A.; Paweska, J. Rift Valley fever virus(Bunyaviridae: Phlebovirus): an update on pathogenesis, molecular epidemiology, vectors, diagnostics and prevention. *Vet Res.* **2010,** *41* (6), 61.
22. Boshra, H.; Lorenzo, G.; Busquets, N.; Brun, A. Rift valley fever: recent insights into pathogenesis and prevention. *J Virol.* **2011,** *85* (13), 6098-105.
23. Chevalier, V. Relevance of Rift Valley fever to public health in the European Union. *Clin Microbiol Infect.* **2013,** *19* (8), 705-8.
24. Brustolin, M.; Talavera, S.; Nunez, A.; Santamaria, C.; Rivas, R.; Pujol, N.; Valle, M.; Verdun, M.; Brun, A.; Pages, N.; Busquets, N. Rift Valley fever virus and European mosquitoes: vector competence of Culex pipiens and Stegomyia albopicta (= Aedes albopictus). *Med Vet Entomol.* **2017,** *31* (4), 365-372.
25. Bouloy, M.; Weber, F. Molecular biology of rift valley Fever virus. *Open Virol J.* **2010,** *4*, 8-14.
26. Kreher, F.; Tamietti, C.; Gommet, C.; Guillemot, L.; Ermonval, M.; Failloux, A. B.; Panthier, J. J.; Bouloy, M.; Flamand, M. The Rift Valley fever accessory proteins NSm and P78/NSm-GN are distinct determinants of virus propagation in vertebrate and invertebrate hosts. *Emerg Microbes Infect.* **2014,** *3* (10), e71.
27. Gerrard, S. R.; Nichol, S. T. Synthesis, proteolytic processing and complex formation of N-terminally nested precursor proteins of the Rift Valley fever virus glycoproteins. *Virology.* **2007,** *357* (2), 124-33.
28. Borrego, B.; Lorenzo, G.; Mota-Morales, J. D.; Almanza-Reyes, H.; Mateos, F.; Lopez-Gil, E.; de la Losa, N.; Burmistrov, V. A.; Pestryakov, A. N.; Brun, A.; Bogdanchikova, N. Potential application of silver nanoparticles to control the infectivity of Rift Valley fever virus in vitro and in vivo. *Nanomedicine.* **2016,** *12* (5), 1185-92.
29. Lorenzo, G.; Lopez-Gil, E.; Ortego, J.; Brun, A. Efficacy of different DNA and MVA prime-boost vaccination regimens against a Rift Valley fever virus (RVFV) challenge in sheep 12 weeks following vaccination. *Veterinary Reaseacrh.* **2018,** *49* (1), 21.
30. Faburay, B.; LaBeaud, A. D.; McVey, D. S.; Wilson, W. C.; Richt, J. A. Current Status of Rift Valley Fever Vaccine Development. *Vaccines (Basel).* **2017,** *5* (3).
31. Dalrymple, J.; Hasty, S. E.; Kakach, L. T.; Collett, M. S., Mapping protective determinants of Rift Valley fever virus using recombinant vaccinia viruses. In *Vaccines 89*, Brown F., C. R. M., Ginsberg H.S., Lerner R.A. , Ed. Cold Spring Harbor Laboratory New York, 1989; pp 371-375.
32. Gerrard, S. R.; Nichol, S. T. Characterization of the Golgi retention motif of Rift Valley fever virus G(N) glycoprotein. *J Virol.* **2002,** *76* (23), 12200-10.

33. Bhardwaj, N.; Heise, M. T.; Ross, T. M. Vaccination with DNA plasmids expressing Gn coupled to C3d or alphavirus replicons expressing gn protects mice against Rift Valley fever virus. *PLoS Negl Trop Dis.* **2010,** *4* (6), e725.
34. Kortekaas, J.; Antonis, A. F.; Kant, J.; Vloet, R. P.; Vogel, A.; Oreshkova, N.; de Boer, S. M.; Bosch, B. J.; Moormann, R. J. Efficacy of three candidate Rift Valley fever vaccines in sheep. *Vaccine.* **2012,** *30* (23), 3423-9.
35. Busquets, N.; Lorenzo, G.; Lopez-Gil, E.; Rivas, R.; Solanes, D.; Galindo-Cardiel, I.; Abad, F. X.; Rodriguez, F.; Bensaid, A.; Warimwe, G.; Gilbert, S. C.; Domingo, M.; Brun, A. Efficacy assessment of an MVA vectored Rift Valley Fever vaccine in lambs. *Antiviral Res.* **2014,** *108*, 165-72.
36. Caplen, H.; Peters, C. J.; Bishop, D. H. Mutagen-directed attenuation of Rift Valley fever virus as a method for vaccine development. *J Gen Virol.* **1985,** *66 (Pt 10)*, 2271-7.
37. Urry, D. W. Entropic elastic processes in protein mechanisms. I. Elastic structure due to an inverse temperature transition and elasticity due to internal chain dynamics. *J Protein Chem.* **1988,** *7* (1), 1-34.
38. Urry, D. W. Molecular Machines: How Motion and Other Functions of Living Organisms Can Result from Reversible Chemical Changes. *Angewandte Chemie International Edition in English.* **1993,** *32* (6), 819-841.
39. Takahashi, Y.; Gehoh, M.; Yuzuriha, K. Structure refinement and diffuse streak scattering of silk (Bombyx mori). *Int J Biol Macromol.* **1999,** *24* (2-3), 127-38.
40. Asakura, T.; Yao, J.; Yamane, T.; Umemura, K.; Ulrich, A. S. Heterogeneous structure of silk fibers from Bombyx mori resolved by 13C solid-state NMR spectroscopy. *J Am Chem Soc.* **2002,** *124* (30), 8794-5.
41. Lopez-Gil, E.; Lorenzo, G.; Hevia, E.; Borrego, B.; Eiden, M.; Groschup, M.; Gilbert, S. C.; Brun, A. A single immunization with MVA expressing GnGc glycoproteins promotes epitope-specific CD8+-T cell activation and protects immune-competent mice against a lethal RVFV infection. *PLoS Negl Trop Dis.* **2013,** *7* (7), e2309.